HHS Public Access

Author manuscript

Nat Biotechnol. Author manuscript; available in PMC 2016 May 14.

Published in final edited form as:

Nat Biotechnol. 2011 March ; 29(3): 267–272. doi:10.1038/nbt.1788.

Generation of anterior foregut endoderm from human embryonic and induced pluripotent stem cells

Michael D Green[1], **Antonia Chen**[1], **Maria-Cristina Nostro**[2], **Sunita L d'Souza**[1], **Christoph Schaniel**[1], **Ihor R Lemischka**[1], **Valerie Gouon-Evans**[1], **Gordon Keller**[2], and **Hans-Willem Snoeck**[1]

[1]Department of Gene and Cell Medicine and Black Family Stem Cell Institute, Mount Sinai School of Medicine, New York, New York, USA.

[2]Division of Stem Cell and Developmental Biology and McEwen Centre for Regenerative Medicine, Ontario Cancer Institute, Toronto, Ontario, Canada.

Abstract

Directed differentiation of human embryonic stem (hES) cells and human induced pluripotent stem (hiPS) cells captures *in vivo* developmental pathways for specifying lineages *in vitro*, thus avoiding perturbation of the genome with exogenous genetic material. Thus far, derivation of endodermal lineages has focused predominantly on hepatocytes, pancreatic endocrine cells and intestinal cells[1–5]. The ability to differentiate pluripotent cells into anterior foregut endoderm (AFE) derivatives would expand their utility for cell therapy and basic research to tissues important for immune function, such as the thymus; for metabolism, such as thyroid and parathyroid; and for respiratory function, such as trachea and lung. We find that dual inhibition of transforming growth factor (TGF)-β and bone morphogenic protein (BMP) signaling after specification of definitive endoderm from pluripotent cells results in a highly enriched AFE population that is competent to be patterned along dorsoventral and anteroposterior axes. These findings provide an approach for the generation of AFE derivatives.

Directed differentiation of pluripotent stem cells into a variety of cell types opens a promising avenue for cell replacement therapy and provides a powerful tool for basic research[4]. ES cells are derived from the inner cell mass of the blastocyst and can be maintained in a pluri-potent state by defined conditions. Furthermore, adult somatic cells can be reprogrammed into a pluripotent state (hiPS cells), paving the way for the generation of patient-specific pluripotent cells[6].

Correspondence should be addressed to H.-W.S. (hans.snoeck@mssm.edu)..

AUTHOR CONTRIBUTIONS

M.D.G. performed all experiments with assistance of A.C. M.-C.N., V.G.-E., S.L.S. and G.K. advised and assisted with induction of definitive endoderm. S.L.S., I.R.L. and C.S. generated and characterized the hiPS lines, respectively. M.D.G. and H.-W.S. designed the experiments and wrote the manuscript.

Supplementary information is available on the Nature Biotechnology website.

COMPETING FINANCIAL INTERESTS

The authors declare competing financial interests: details accompany the full-text HTML version of the paper at http://www.nature.com/naturebiotechnology/.

Most efforts at generating endoderm derivatives from human pluripotent cells have focused on midgut (pancreatic endocrine cells) and posterior foregut (hepatocyte) cell types[1–4,7]. However, several clinically relevant cell types originate from AFE, the most rostral aspect of the endoderm. The caudal region of the AFE gives rise to trachea and lung[8]. The generation of respiratory tissue may allow cellular replacement therapies for respiratory disease. Rostral to the lung field is the pharyngeal endoderm, which forms four paired outcroppings, called pharyngeal pouches[9]. These develop into specific organs: eustachian tube and tympanic membrane (first pouch), palatine tonsils (second pouch), thymus (anterior third pouch), parathyroids (dorsal third and fourth pouch) and parafollicular C cells of the thyroid (fourth pouch). The thyroid body develops from the floor of the pharynx[9]. Several of these organs are excellent candidates for cellular replacement therapy. The thymus is the site of production of T lymphocytes[10]. Thymic function is severely affected by allogeneic hematopoietic stem cell transplantation, because of both pretransplant conditioning regimens and post-transplant graft-versus-host disease, leading to profound defects in T-cell reconstitution[11]. As the thymus involutes with age, older transplant recipients would particularly benefit from thymic replacement therapy. In addition, the thymus is congenitally absent in nude/severe combined immuno-deficient (SCID) and DiGeorge syndromes[10]. Moreover, autoimmune, congenital or acquired hypothyroidism and genetic or iatrogenic hypoparathyroidism may be treatable by replacement with tissues derived from ES or iPS cells.

Efforts at generating AFE-derived cells have met with little success, although upregulation of thymus[12,13], thyroid[14], parathyroid[15] or lung markers[16] in differentiating ES cells either after specification of definitive endoderm or in mixed-lineage embryoid bodies has been reported. However, these reports relied on drug selection, did not quantify the efficiency of induction or did not determine the presence of alternative lineages. Because cell fate is established through sequential and increasingly lineage-restricted progenitors[4,8], we hypothesized that the failure to specify these cell types with high efficiency *in vitro* is due to the inability to induce AFE from endoderm. Therefore, we developed a strategy to generate AFE from human pluripotent cells.

Definitive endoderm, one of the three germ layers of the embryo proper, is induced from ES cells by high concentrations of activin A, mimicking nodal signaling during gastrulation[6]. Examination of this process in the hES cell line HES2 by quantitative PCR revealed a transcriptional cascade in which the primitive streak marker *MIXL1* and then the endodermal transcription factors *SOX17* and *FOXA2* are upregulated (**Fig. 1a**)[1,2,7,8,17]. After 4 d of exposure to activin A, >95% of the cells expressed the definitive endoderm markers CXCR4, c-KIT and EPCAM (**Fig. 1b**)[17]. After gastrulation, the definitive endoderm forms a tube with distinct anteroposterior axis identity[8]. Within definitive endoderm, the pluripotency marker *SOX2* reemerges as a foregut marker, whereas *CDX2* identifies hindgut[18]. After activin A removal at day 5 of culture, we observed an increase in both *CDX2* and *SOX2* expression (**Fig. 1a**), suggesting the generation of a mixture of anterior and posterior definitive endoderm. Therefore, we examined which signals added after induction of definitive endoderm favored anterior ($SOX2^+$) and suppressed posterior ($CDX2^+$) endoderm generation.

Following the generation of a $CXCR4^+EPCAM^+$ population in embryoid bodies exposed to activin A, the embryoid bodies were dissociated and plated as a monolayer. We tested the addition of 24 combinations of morphogens and inhibitors at day 5 (**Fig. 1c**), and used expression of *FOXA2*, *SOX2*, *CDX2*, *TBX1* (endoderm anterior to the stomach)[9,18,19] and *PAX9* (pharyngeal endoderm)[10,19] as readouts of cellular identity at day 9 of culture. Only in the combined presence of NOGGIN, a physiological inhibitor of BMP signaling, and SB-431542, a pharmacological inhibitor of activin A/nodal and TGF-β signaling, was *SOX2* expression induced, *CDX2* expression suppressed and *FOXA2* expression maintained. Furthermore, only this condition induced strong expression of *TBX1* and *PAX9* (**Fig. 1c**). During the activin A–induction stage, cell number increased 4.5- ± 1.9-fold, and during the NOGGIN/SB-431542 stage, the cells expanded another 1.4- ± 0.4-fold. Notably, NOGGIN/SB-431542 treatment was equally potent in two hiPS cell lines (HDF2 and HDF9), with induction of *SOX2*, *PAX9* and *TBX1* (**Supplementary Fig. 1**). Multiple FGF family members and WNT3a, consistent with their functions in development[5,7,20], posteriorized definitive endoderm, as shown by increased *CDX2* expression (**Fig. 1c**). However, WNT antagonism through addition of soluble Frizzled-related protein 3 (sFRP3) was not sufficient to induce *SOX2* (**Fig. 1c**). Furthermore, sFRP3 did not synergize with NOGGIN/SB-431542, and even appeared detrimental for the induction of *PAX9* and *SOX2* (**Fig. 1d**). The timing of the addition of NOGGIN/SB-431542 was critical, as only treatment immediately after the generation of a uniform $CXCR4^+c\text{-}KIT^+$ or $CXCR4^+EPCAM^+$ population at day 5/6 induced a $SOX2^+FOXA2^+$ population at day 9. Earlier administration abrogated gastrulation, and later administration failed to downregulate the posterior marker *CDX2* (data not shown).

FOXA2 is also expressed in the notochord (mesoderm), and *FOXA2* and *SOX2* are co-expressed by the hindbrain floorplate (neurectoderm)[21,22]. Furthermore, direct application of NOGGIN/SB-431542 to hES cells without prior endoderm induction by activin A leads to a neuroectodermal fate[23]. Therefore, we assayed for the presence of these alternative fates. As expected, the neuroectodermal marker *PAX6* was expressed in cultures where NOGGIN/SB-431542 was added at day 1, whereas *BRACHYURY*, a marker of the notochord and of gastrulating cells, was expressed during early endoderm induction (**Fig. 1e**). Neither *BRACHYURY* nor *PAX6* were expressed in definitive endoderm exposed to NOGGIN/SB-431542 (**Fig. 1e**), indicating that NOGGIN/SB-431542 treatment of activin A–induced definitive endoderm specifies only AFE.

To further assess whether the NOGGIN/SB-431542-induced endodermal cells were distinct from previously described endodermal lineages, we compared day 9 NOGGIN/SB-431542-treated cultures with day 9 cultures grown under conditions favoring a hepatic (posterior foregut) fate. The latter has been previously shown to require BMP-4 and bFGF after activin A induction of endoderm[2]. The expression of *CDX2*, the hindgut marker *EVX1*, the liver markers *CREB313* and *CEBPA*, as well as *ODD1*, a stomach domain marker[18], was higher in the ‘hepatic’ conditions than in the NOGGIN/SB-431542 conditions, and the reverse was true for the anterior markers *TBX1*, *PAX9*, *SOX2* and *FGF8*, a marker within the endoderm specific for pharyngeal pouch endoderm[24] (**Fig. 1f**). Therefore, NOGGIN/SB-431542 treatment specifies AFE cells that are distinct from those specified in hepatic conditions.

Application of NOGGIN/SB-431542 to activin A–induced definitive endoderm yielded colonies of densely packed cells surrounding an empty lumen-like or cyst-like opening. More than 90% of the cells were found in such colonies if plated at high density. Virtually all cells co-expressed SOX2 and FOXA2 (**Fig. 2a**, for HES2 cells, **Fig. 2b** for HDF9 iPS cells, **Supplementary Fig. 2a** for HDF9 and HDF2 hiPS cells, and **Supplementary Fig. 2b** for HES2 cells in Matrigel culture), although rare cells expressed only FOXA2 (**Fig. 2a** and **Supplementary Fig. 2a**, arrows). All colonies stained positive for TBX1, PAX9 and the pharyngeal endoderm marker FOXG1 (**Fig. 2a**, HES2 cells). The typical colonies observed in NOGGIN/SB-431542-treated cultures were never seen when cells were cultured in media without added factors (**Supplementary Fig. 2c**). In these conditions, >95% of cells expressed FOXA2, but only rarely were $SOX2^{+}FOXA2^{+}$ cells observed (**Supplementary Fig. 2c**, arrows). Colonies with this morphology were also never observed in hepatic conditions (**Supplementary Fig. 2d**). Comparative immunofluorescence analysis of HES2-derived endodermal cells cultured in parallel in either NOGGIN/SB-431542 or hepatic conditions revealed that only NOGGIN/SB-431542 cultures were characterized by strong SOX2, PAX9 and TBX1 expression (**Supplementary Fig. 2d**).

Collectively, these expression data show that NOGGIN/SB-431542 specifies a highly enriched population of cells with AFE phenotype in activin A–induced definitive endoderm. These findings are consistent with the fact that mice null for the BMP antagonist *Chordin* display anterior truncations[25] and with the observation that activin A–induced endoderm contains a large fraction of $CDX2^{+}$ posterior endoderm (**Fig. 1a**).

To determine the potential *in vivo* of cells cultured in NOGGIN/SB-431542 conditions, we transplanted 10^{6} cells under the kidney capsule of NOD/SCID*Il2rg*$^{-/-}$ mice. Whereas undifferentiated HES2 cells generated teratomas containing cells derived from all three germ layers (**Fig. 3a**), NOGGIN/SB-431542-treated cells produced growths lacking identifiable ectodermal or mesodermal elements (**Fig. 3b**). We observed multiple luminal structures, lined either by pseudostratified epithelium (typical of upper airway epithelium) or a more disorganized epithelium containing one to three layers of nuclei (**Fig. 3b**). The latter consistently stained for surfactant protein-C (SFTPC), a marker specific for type II alveolar cells in the lung (**Fig. 3c** and **Supplementary Fig. 3a**). In hES cell–derived teratomas, no SFTPC staining was observed (data not shown). The remainder of the cells stained almost uniformly for FOXA2. However, except in the luminal structures, FOXA2 was confined to the cytoplasm, possibly owing to differentiation into $FOXA2^{-}$ terminal AFE derivatives or to abnormal FOXA2 regulation in a xenograft (**Fig. 3c**). Islands of cells expressing PAX9, as well as rare regions showing discrete nuclear speckles of AIRE (specific for medullary thymic epithelial cells[10]), were also detected (**Fig. 3c**). In hES-derived teratomas, PAX9 was only observed in zones of cartilage formation and AIRE expression was not observed (data not shown). Collectively, these data suggest that the developmental potential of NOGGIN/SB-431542-induced definitive endoderm is largely limited to AFE derivatives in these conditions.

Next, we attempted to further differentiate these cells. AFE undergoes dorsoventral patterning, resulting in specification of lung buds, trachea and pharyngeal pouches in response to WNT, BMP and FGF signals from the ventral mesoderm[10,26]. At this stage,

SOX2 expression remains higher dorsally, whereas *NKX2.1* (lung and thyroid field[8,26]), *NKX2.5* (transiently expressed in the ventral pharyngeal endoderm[27]) and *PAX1* (within endoderm specifically expressed in the pharyngeal pouches[28]) are specific ventral markers. Extended treatment with NOGGIN/SB-431542 until day 13 resulted in continued expression of *SOX2*, suggestive of a dorsal fate (**Fig. 3d**) and consistent with the fact that Noggin is expressed dorsally in the AFE, whereas BMP4 is expressed ventrally[26]. In contrast, replacing NOGGIN/SB-431542 with WNT3a, KGF, FGF10, BMP4 and EGF (all factors, WKFBE) at day 7 of culture resulted in lower expression of *SOX2* and induced the ventral markers *NKX2.1*, *PAX1* and *NKX2.5* at day 13 (**Fig. 3d** for HES cells and **Supplementary Fig. 3a,b** for HDF2 and HDF9 hiPS cells). Expression of the early thyroid marker, *PAX8*, was not observed, however, suggesting that *NKX2.1* induction is indicative of commitment to a lung, rather than a thyroid, fate (data not shown). Furthermore, *P63*, a marker of airway progenitor cells[26], was strongly induced (**Fig. 3d**), and the vast majority of the cells expressed the epithelial marker EPCAM (**Supplementary Fig. 3c**). Addition of individual factors was not sufficient for this transcriptional induction (data not shown). Furthermore, only prior exposure to NOGGIN/SB-431542, and not to the hepatic cocktail or to media alone enabled subsequent upregulation of *PAX1*, *NKX2.1* and *NKX2.5* by WKFBE (**Fig. 3e**), demonstrating that NOGGIN/SB-431542 treatment of activin A–induced definitive endoderm is required for differentiation toward a ventral AFE fate. Timing of the WKFBE ventralization stimulus was critical, as only cultures treated at day 7, but not at day 9, were competent to express *NKX2.1*, *PAX1* and *NKX2.5* (data not shown). At this time, 92 ± 2% of the cells were $FOXA2^{+}SOXA2^{+}$ (**Fig. 3f,g**). Immunofluorescence revealed that after induction in WKFBE, 37 ± 6% of cells expressed NKX2.1 (**Fig. 3h** and **Supplementary Fig. 3d**). During NOGGIN/SB-431542 followed by WKFBE treatment of activin A–induced endoderm, cells expanded an additional 8.95- ± 3.3-fold (**Fig. 3g**). Thus, NOGGIN/SB-431542-induced AFE is uniquely competent to respond to ventralization signals *in vitro*.

Exposure of NOGGIN/SB-431542-induced AFE to WKFBE did not result in expression of terminal differentiation markers for thymus, parathyroid, thyroid or lung at day 13 or day 19 of culture (data not shown). As these cells had the potential to give rise to $SFTPC^{+}$ cells *in vivo*, we attempted to achieve lung specification *in vitro*. Consistent with a critical role for retinoic acid in early lung development[29], addition of retinoic acid to the WKFBE cocktail decreased the expression of the pharyngeal pouch marker *PAX1*, but increased *FOXP2*, *NKX2.1*, *GATA6* and *FOXJ1*, a constellation of markers suggestive of a lung fate[26] (**Fig. 4a**). To enhance *SFTPC* induction, we added combinations of signaling agonists and antagonists at day 11 to AFE ventralized in the presence of retinoic acid. Among the >400 combinations examined, WNT3a + FGF10 + FGF7 induced high levels of *SFTPC* mRNA (**Fig. 4b**) at day 19, consistent with the developmental observations that FGF10 and Wnt signaling are critical for distal lung development[26]. To assess whether NOGGIN/SB-431542-induced AFE could generate pharyngeal pouch derivatives, we sought to pattern the cultures ventralized with WKFBE in the absence of retinoic acid. Consistent with the requirement of sonic hedgehog (SHH) and FGF8 for parathyroid development[30], addition of FGF8 or SHH to AFE cultures induced the parathyroid-specific marker *GCM2* (**Fig. 4b**). The effects of SHH and FGF8 were not additive, mirroring *in vivo* epistasis studies showing that *Shh* is upstream of *Fgf8* in mouse pharyngeal pouch development[30]. Although we did

not test all temporal and signaling permutations exhaustively, these data suggest that NOGGIN/SB-431542-induced cells are capable of differentiating into downstream lineages, including the lung field and pharyngeal pouches.

Collectively, our data show that dual inhibition of BMP and TGF-β signaling in hES/hiPS cell-derived definitive endoderm specifies a highly enriched AFE population, providing an *in vitro* approach for the directed differentiation of human pluripotent cells into cell types and tissues derived from the AFE *in vivo*.

ONLINE METHODS

Cells and culture conditions

hESC (HES2, National Institutes of Health code ES02 from ES Cell International; passages 25–33) were cultured on mouse embryonic fibroblasts plated at 8,000–12,000 cells/cm^2. A medium of DMEM/F12, 20% knockout serum replacement (Gibco), 0.1 mM β-mercaptoethanol (Sigma-Aldrich), and 20 ng/ml FGF-2 (R&D) was changed daily. Cells were passaged with trypsin, washed and replated at a dilution of 1:5 to 1:10. HDF2 and HDF9, hiPS cell lines, were cultured as hES2. hES and hiPS cultures were maintained in a 5% CO_2/air environment, and hES differentiations were maintained in a 5% CO_2/5% O_2/90% N_2 environment.

Endoderm induction

Mouse embryonic fibroblasts were depleted by a 24 h passage on Matrigel (Gibco) with Y-27632 (10 μM), and embryoid bodies were formed on low-adherence dishes (Costar). During embryoid body formation and differentiation, HES2 cells were reseeded at the same concentration (1:1 dilution), whereas HDF2 and HDF9 required a higher seeding (2:1–4:1 concentration) for efficient endoderm generation. Differentiations were performed in a medium of DMEM/F12 (Invitrogen) supplemented with N2 (Gibco), B27 (Gibco), ascorbic acid (50 μg/ml, Sigma), Glutamax (2 mM, Invitrogen), monothioglycerol (0.4 μM, Sigma). The following concentrations of factors were used for primitive streak formation, endoderm induction, anterior/pharyngeal endoderm induction, and subsequent anterior posterior and dorsoventral patterning: human BMP-4, 1 ng/ml and 10 ng/ml; human bFGF, 2.5 ng/ml; human activin A, 100 ng/ml; human NOGGIN, 200 ng/ml; Y-27632, 1 μM; SB-431542, 10 μM; human FGF10, 10 ng/ml; human FGF7, 10 ng/ml; murine EGF 20 ng/ml; and human WNT3a, 100 ng/ml. Hepatic conditions were as previously described[2] and contain BMP-4, 50 ng/ml; bFGF, 10 ng/ml; VEGF, 10 ng/ml; HGF, 10 ng/ml; TGFα, 20 ng/ml; dexamethasone, 40 ng/ml. All factors were purchased from R&D systems, except SB-431542 and Y-27632, which are from Tocris, and dexamethasone (Sigma). The factors were added in the following sequence: day 1, Y-27632; days 1–5, BMP4, bFGF and activin A; days 5–9, NOGGIN and SB-431542; days 7–19 WNT3a, FGF10, BMP4, FGF7 and EGF. For hepatic differentiation, factors were added in the following sequence: day 1, Y-27632; days 1–5, BMP4, bFGF and activin A; days 5–9, dexamethasone, bFGF, HGF, VEGF, EGF, TGFa and BMP4. For some experiments, 500 μM all-trans retinoic acid (Sigma) was added to the cultures. At day 5, embryoid bodies were trypsinized (Gibco) and plated at 10,000–50,000 cells/cm^2 in gelatin-coated, tissue culture–treated dishes (Fisher).

The day 11 screen of morphogens (**Fig. 3h**) included pairwise and some higher order of magnitude additions of FGFS (FGF10 + FGF7) (R&D Systems), SU-5402 (EMD Chemicals), Wnt5a (R&D Systems), WNT3a (R&D Systems), sFRP1 (R&D Systems), BMP4, NOGGIN, SHH (R&D Systems), cyclopamine (EMD Chemicals), SB-431542, TGF-β1 (R&D Systems), DAPT (EMD Chemicals), retinoic acid (Sigma), DEAB (Sigma), EGF (R&D Systems), tyrophastin AG-1478 (EMD Chemicals) and WP1066 (EMD Chemicals).

Quantitative PCR

Total RNA was extracted using Trizol (Invitrogen), phase lock tubes (5′ Prime) and the RNeasy kit (Qiagen). We treated 1–2 μg of total RNA with DNase I (Qiagen) and reverse transcribed it using random hexamers and Superscript III (Invitrogen). Amplified material was detected using SybrGreen (Invitrogen). Real-time quantitative PCR was performed on ABI 7900HT thermocycler (Applied Biosystems), with a 10-min step at 95 °C followed by 40 cycles of 95 °C for 15 s and 60 °C for 1 min. All experiments were done in triplicate with SYBR GreenER quantitative PCR SuperMix (Invitrogen). Denaturing curves for each gene were used to confirm homogeneity of the DNA product. Absolute quantification was obtained in relation to a standard curve of genomic DNA dilution series. Quantified values for the gene of interest were normalized against input determined by the housekeeping genes *GAPDH* and β-*ACTIN*. qPCR for each culture well was performed in triplicate. Primer sequences are listed in **Supplementary Table 1**.

Flow cytometry

Day 5 embryoid bodies or day 13 monolayer cultures were dissociated with trypsin/EDTA (2 min). The cells were stained with directly conjugated CXCR4 (Invitrogen), c-KIT (BD Biosciences) and EPCAM (BD Biosciences) in IMDM complemented with 10% serum. Cells were analyzed on a LSRII. Flowjo software (Tree Star) was used for all analyses.

Immunofluorescence

Day-7, -9 or -13 cultures were fixed with fresh paraformaldehyde (4%) for 30 min at 25 °C and then washed in PBS. The cells were permeabilized and blocked in a solution with 0.1% saponin, 0.1% BSA, 10% FCS (Gemstar) and 10% fetal donkey serum (Jackson Immunofluorescence). For three-dimensional cultures, cells were embedded at day 5 in Matrigel using the “embedded” and “on-top” assays, as previously described[31]. Cultures were embedded in Optimal Cutting Temperature (OCT, Tissue Tek) at day 9, extracted, sectioned and processed as above. Primary antibodies were added overnight, and include PAX-9 (Abcam), TBX1 (Abcam), SOX2 (Stemgent, Santa Cruz), CDX2 (Abcam), NKX2-1 (Invitrogen) and AIRE (Santa Cruz). Cells were washed and incubated with donkey anti-mouse whole IgG-Dylight488, donkey anti-goat whole IgG-Cy3, and donkey anti-rabbit whole IgG-Cy5 for 1 h. The cells were washed, and nuclei were stained with DAPI (Invitrogen). Stains were visualized using a fluorescence microscope (Leica DMI 4000B, Wetzlar, Germany). This instrument was fitted with a DFC340 Fx Monochrome Cooled Digital Camera for fluorescent acquisition (Leica) and variable objective lenses (5×–40×) were used. Filter models: A4 UV, 11504135; GFP, 11532366; YFP 1153267; RFP,

11513894; CY3, 11600231. Exposure settings varied, but were set based on hepatic-specified cultures differentiated and stained in parallel. Images were acquired using Leica Application Suite Advanced Fluorescence Software Package AF6000 (Leica) in PBS at 25 °C. Images are shown without rendering or deconvolution. Images were digitally processed using Adobe Photoshop CS4 (Adobe) in accordance with Nature Publishing Guidelines by altering only contrast and brightness, and these manipulations were performed on hepatic specified and experimental conditions simultaneously. Quantification was performed by counting a minimum of ten random fields at 20× magnification. On most panels, the magnification by the lens objective is listed.

Mice

NOD.Cg-*Prkdc*^{scid}*Il2rg*^{tm1Wjl}/SzJ (NOD/SCID*Il2rg*$^{-/-}$) mice were purchased from Jackson Laboratory. Animals were kept in a specific pathogen-free facility. Experiments and animal care were performed in accordance with the Mount Sinai Institutional Animal Care and Use Committee. One million cells were injected under the kidney capsule. Outgrowths were excised, embedded in OCT and analyzed using hematoxylin and eosin stains for morphology or immunofluorescence for specific antigens as above.

Statistical analysis

For statistical analysis, unpaired *t*-test and when more than two groups were compared, one-way ANOVA was used. Results are expressed as mean ± s.e.m.

Supplementary Material

Refer to Web version on PubMed Central for supplementary material.

ACKNOWLEDGMENTS

This work was supported by NYSTEM grant NO8G-422 to H.-W.S.

References

1. D'Amour KA, et al. Production of pancreatic hormone-expressing endocrine cells from human embryonic stem cells. Nat. Biotechnol. 2006; 24:1392–1401. [PubMed: 17053790]
2. Gouon-Evans V, et al. BMP-4 is required for hepatic specification of mouse embryonic stem cell-derived definitive endoderm. Nat. Biotechnol. 2006; 24:1402–1411. [PubMed: 17086172]
3. Cai J, et al. Directed differentiation of human embryonic stem cells into functional hepatic cells. Hepatology. 2007; 45:1229–1239. [PubMed: 17464996]
4. Murry CE, Keller G. Differentiation of embryonic stem cells to clinically relevant populations: lessons from embryonic development. Cell. 2008; 132:661–680. [PubMed: 18295582]
5. Spence JR, et al. Directed differentiation of human pluripotent stem cells into intestinal tissue in vitro. Nature. 2010; 470:105–109. [PubMed: 21151107]
6. Yamanaka S. A fresh look at iPS cells. Cell. 2009; 137:13–17. [PubMed: 19345179]
7. Gadue P, Huber TL, Paddison PJ, Keller GM. Wnt and TGF-beta signaling are required for the induction of an in vitro model of primitive streak formation using embryonic stem cells. Proc. Natl. Acad. Sci. USA. 2006; 103:16806–16811. [PubMed: 17077151]
8. Zorn AM, Wells JM. Vertebrate endoderm development and organ formation. Annu. Rev. Cell Dev. Biol. 2009; 25:221–251. [PubMed: 19575677]

9. Graham A. Deconstructing the pharyngeal metamere. J. Exp. Zoolog. B Mol. Dev. Evol. 2008; 310:336–344.
10. Rodewald HR. Thymus organogenesis. Annu. Rev. Immunol. 2008; 26:355–388. [PubMed: 18304000]
11. Jenq RR, van den Brink MR. Allogeneic haematopoietic stem cell transplantation: individualized stem cell and immune therapy of cancer. Nat. Rev. Cancer. 2010; 10:213–221. [PubMed: 20168320]
12. Lai L, Jin J. Generation of thymic epithelial cell progenitors by mouse embryonic stem cells. Stem Cells. 2009; 27:3012–3020. [PubMed: 19824081]
13. Hidaka K, et al. Differentiation of pharyngeal endoderm from mouse embryonic stem cell. Stem Cells Dev. 2010; 19:1735–1743. [PubMed: 20230268]
14. Lin RY, Kubo A, Keller GM, Davies TF. Committing embryonic stem cells to differentiate into thyrocyte-like cells in vitro. Endocrinology. 2003; 144:2644–2649. [PubMed: 12746328]
15. Bingham EL, Cheng SP, Woods Ignatoski KM, Doherty GM. Differentiation of human embryonic stem cells to a parathyroid-like phenotype. Stem Cells Dev. 2009; 18:1071–1080. [PubMed: 19025488]
16. Wang D, Haviland DL, Burns AR, Zsigmond E, Wetsel RA. A pure population of lung alveolar epithelial type II cells derived from human embryonic stem cells. Proc. Natl. Acad. Sci. USA. 2007; 104:4449–4454. [PubMed: 17360544]
17. Yasunaga M, et al. Induction and monitoring of definitive and visceral endoderm differentiation of mouse ES cells. Nat. Biotechnol. 2005; 23:1542–1550. [PubMed: 16311587]
18. Sherwood RI, Chen TY, Melton DA. Transcriptional dynamics of endodermal organ formation. Dev. Dyn. 2009; 238:29–42. [PubMed: 19097184]
19. Peters H, Neubüser A, Kratochwil K, Balling R. Pax9-deficient mice lack pharyngeal pouch derivatives and teeth and exhibit craniofacial and limb abnormalities. Genes Dev. 1998; 12:2735–2747. [PubMed: 9732271]
20. Li Y, et al. Sfrp5 coordinates foregut specification and morphogenesis by antagonizing both canonical and noncanonical Wnt11 signaling. Genes Dev. 2008; 22:3050–3063. [PubMed: 18981481]
21. Wood HB, Episkopou V. Comparative expression of the mouse Sox1, Sox2 and Sox3 genes from pre-gastrulation to early somite stages. Mech. Dev. 1999; 86:197–201. [PubMed: 10446282]
22. Weinstein DC, et al. The winged-helix transcription factor HNF-3 beta is required for notochord development in the mouse embryo. Cell. 1994; 78:575–588. [PubMed: 8069910]
23. Chambers SM, et al. Highly efficient neural conversion of human ES and iPS cells by dual inhibition of SMAD signaling. Nat. Biotechnol. 2009; 27:275–280. [PubMed: 19252484]
24. Vitelli F, et al. A genetic link between Tbx1 and fibroblast growth factor signaling. Development. 2002; 129:4605–4611. [PubMed: 12223416]
25. Bachiller D, et al. The role of chordin/Bmp signals in mammalian pharyngeal development and DiGeorge syndrome. Development. 2003; 130:3567–3578. [PubMed: 12810603]
26. Morrisey EE, Hogan BL. Preparing for the first breath: genetic and cellular mechanisms in lung development. Dev. Cell. 2010; 18:8–23. [PubMed: 20152174]
27. Tanaka M, Schinke M, Liao HS, Yamasaki N, Izumo S. Nkx2.5 and Nkx2.6, homologs of Drosophila tinman, are required for development of the pharynx. Mol. Cell. Biol. 2001; 21:4391–4398. [PubMed: 11390666]
28. Wallin J, et al. Pax1 is expressed during development of the thymus epithelium and is required for normal T-cell maturation. Development. 1996; 122:23–30. [PubMed: 8565834]
29. Chen F, et al. A retinoic acid-dependent network in the foregut controls formation of the mouse lung primordium. J. Clin. Invest. 2010; 120:2040–2048. [PubMed: 20484817]
30. Moore-Scott BA, Manley N. Differential expression fo sonic hedgehog along the anterior-posterior axis regulates patterning of pharyngeal pouch endoderm and pharyngeal endoderm-derived organs. Dev. Biol. 2005; 278:323–335. [PubMed: 15680353]
31. Lee GY, Kenny PA, Lee EH, Bissell MJ. Three-dimensional culture models of normal and malignant breast epithelial cells. Nat. Methods. 2007; 4:359–365. [PubMed: 17396127]

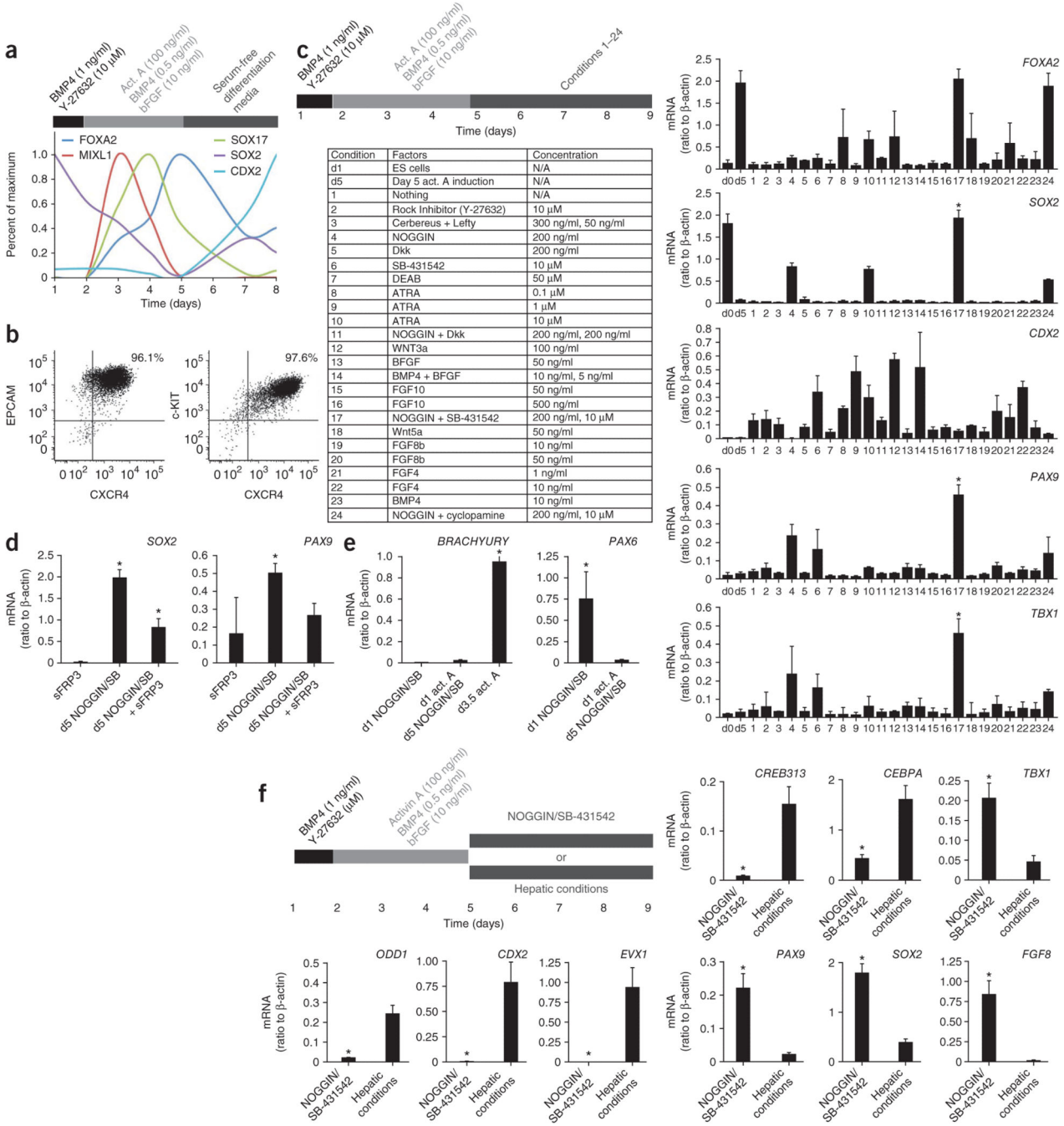

Figure 1.

Induction of AFE markers in NOGGIN/SB-431542-treated definitive endoderm. (**a**) Expression of *FOXA2*, *MIXL1*, *SOX17*, *SOX2* and *CDX2* mRNA during activin A–mediated induction of definitive endoderm in hES cells. Data expressed as quantification of mRNA normalized to β-*ACTIN* (also known as *ACTB*), scaled proportionally to maximum induction. Cytokines were added as indicated on top of the figure (bar). (**b**) Representative flow cytometric analysis of definitive endodermal markers CXCR4, C-KIT and EPCAM at day 5 of activin A induction. Two biologically independent experiments are shown. (**c**)

Expression of *FOXA2*, *SOX2*, *CDX2*, *PAX9* and *TBX1* mRNA on day 9 in cultures treated on day 5 after induction of definitive endoderm (see upper left panel), with the factors listed in the lower left panel ($n = 3$ biological replicates; *, significantly different from all other conditions, $P < 0.0001$; one-way ANOVA). d0, prior to start of differentiation; d5, day 5. (**d**) Expression of *SOX2* and *PAX9* on day 9 in cultures treated on day 5, after induction of definitive endoderm, with NOGGIN/SB-431542 (SB) in the presence or absence of sFRP3 (*, $P < 0.05$, $n = 3$ biological replicates). (**e**) Expression of *BRACHYURY* and *PAX6* mRNA at day 9 in hES cells differentiated as previously described to neurectoderm (day 1 addition of NOGGIN/SB-431542), or after induction of endoderm (endoderm induction until day 5, followed by addition of NOGGIN/SB-431542). For *BRAYCHURY*, day 3.5 hES cells exposed to activin A and undergoing gastrulation served as a positive control (*, $P < 0.0001$, $n = 3$ experiments consisting each of three biological replicates). (**f**) Expression of *ODD1*, *CDX2*, *EVX1*, *CREB313*, *CEBPA*, *TBX1*, *PAX9*, *SOX2* and *FGF8* mRNA in day 9 cultures treated in parallel with either NOGGIN/SB-431542 or cultured in hepatic conditions after induction of definitive endoderm until day 5 ($n = 3$ experiments consisting each of three biological replicates).

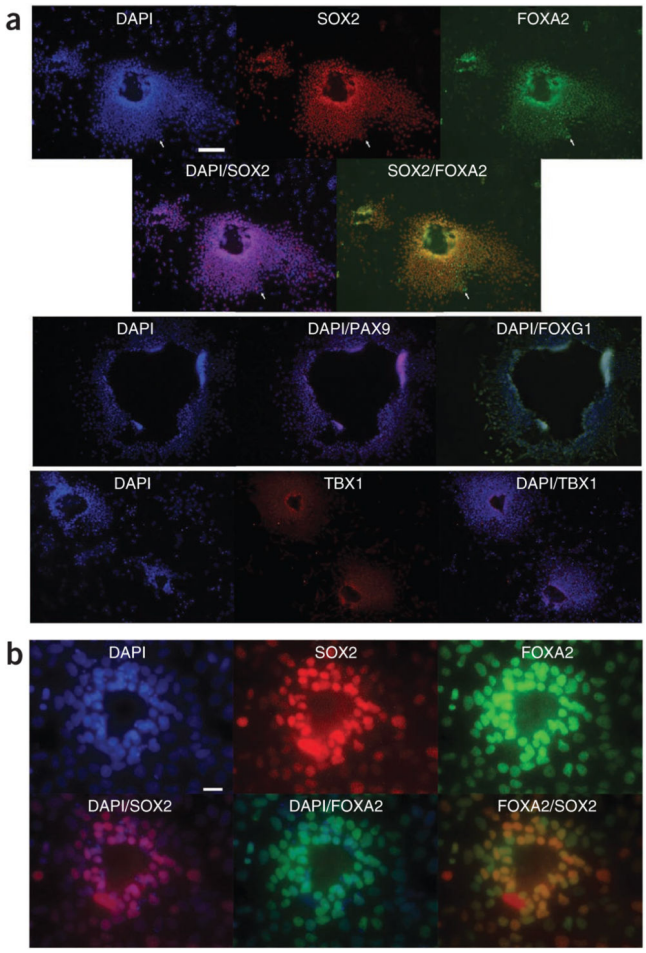

Figure 2.

Immunofluorescence analysis of NOGGIN/SB-431542-treated definitive endoderm. (**a**) Immunofluorescence for FOXA2, SOX2, CDX2, PAX9, FOXG1 and TBX1 of day 9 in HES2 definitive endoderm cultures treated on day 5 with NOGGIN/SB-431542. Scale bar, 50 μm (upper); 100 μm (lower). (**b**) Expression of FOXA2 and SOX2 in HFD9 hiPS cultures in the same conditions. Scale bar, 25 μm.

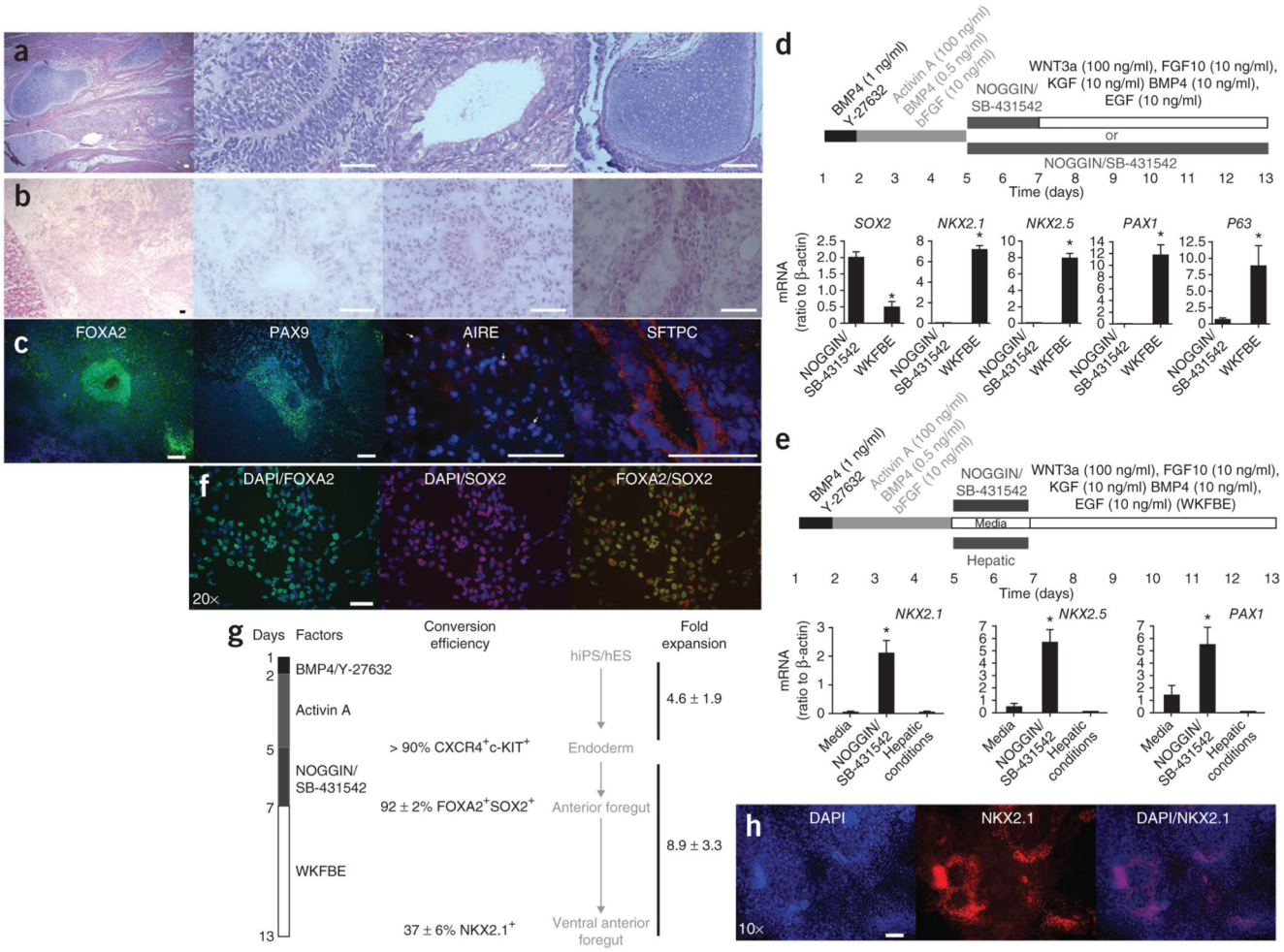

Figure 3.

Functional characteristics of NOGGIN/SB-431542-induced AFE cells. (**a**) H/E staining of a teratoma derived after 5 weeks from HES2 transplanted under the kidney capsule of NOD/SCID*Il2rg*$^{-/-}$ mice. The three right-hand panels show neurectoderm (neural rosette), endoderm (intestinal epithelium) and mesoderm (cartilage), respectively. Scale bar, 50 μ. (**b**) H/E staining of a growth arising 5 weeks after transplantation of NOGGIN/SB-431542-induced AFE cells derived from HES2 cells under the kidney capsule of immunocompromised mice. Scale bar, 50 μm. (**c**) Immunofluorescence analysis of the tissue from b stained for FOXA2, PAX9, AIRE and SFTPC. Scale bar, 50 μm. (**d**) Expression of *SOX2*, *NKX2.1*, *NKX2.5*, *PAX1* and *P63* in HES2-derived cells generated in the two conditions schematically represented on top of the panel ($n = 6$ culture wells from two independent experiments; *, significantly different from NOGGIN/SB-431542; $P < 0.05$) WKFBE: WNT3a, KGF, FGF10, BMP4 and EGF. (**e**) Expression of NKX2.1, NKX2.5 and PAX1 in HES2-derived cells generated in the three conditions schematically represented on top of the panel ($n = 4$ to 6 culture wells from three independent experiments, *, significantly different from the other conditions; $P < 0.05$). (**f**) Expression of FOXA2 (green) and SOX2 (red) 2 d after treatment of activin A–induced definitive endoderm with NOGGIN/SB-431542 (blue, DAPI). Scale bar, 50 μm. (**g**) Schematic overview of the

efficiency of induction of ventral AFE. WKFBE: WNT3a, KGF, FGF10, BMP4 and EGF. (**h**) Immunofluorescence for NKX2.1 in differentiated HDF9 hiPS cells after sequential treatment with activin A, NOGGIN/SB-431542 and WKFBE according to the scheme in **g**. Scale bar, 50 μm.

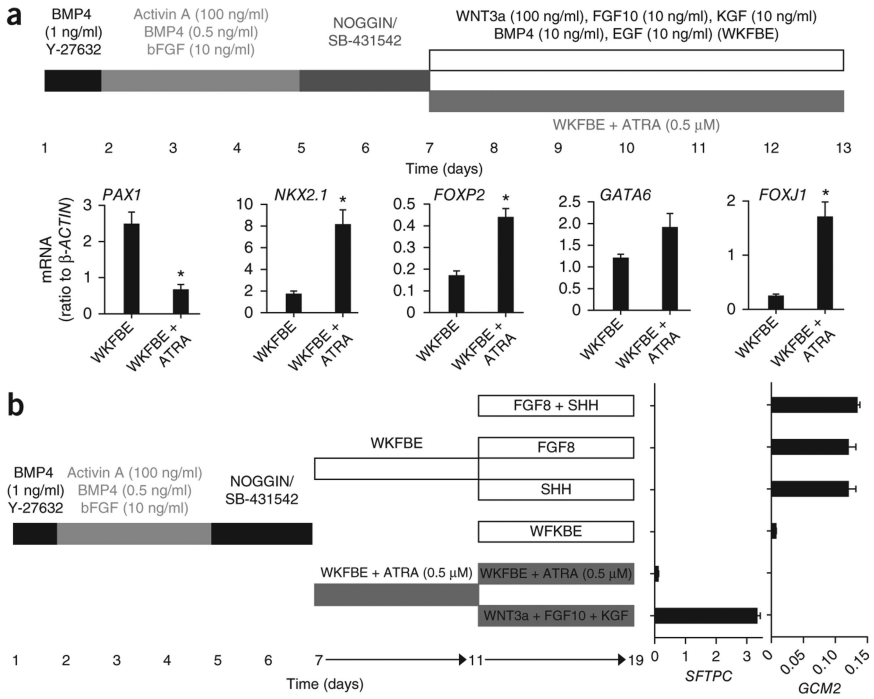

Figure 4.

Induction of lung and pharyngeal pouch markers from ventral AFE generated *in vitro*. (**a**) Expression of *PAX1*, *NKX2.1*, *FOXP2*, *GATA6* and *FOXJ1* in HES2-derived cells generated in the two conditions schematically represented on top of the panel ($n = 4$ to six culture wells from three independent experiments, *, significantly different from WKFBE conditions; $P < 0.05$). WKFBE: WNT3a, KGF, FGF10, BMP4 and EGF. (**b**) Induction of *SFTPC* and *GCM2* mRNA in ventralized AFE in the presence of factors indicated in the figure.